Polymer Bulletin (2024) 81:12841–12865
https://doi.org/10.1007/s00289-024-05304-y

ORIGINAL PAPER

A comparison of controlled release from cyclodextrin mediated and non-mediated hydrogel matrices of Moringa Oleifera gum and carboxymethyl cellulose

Kuljit Kaur[1] · Lakhveer Kaur[1] · Anmol[1] · Mehak Sharma[1] · Rajeev Jindal[2]

Received: 15 November 2023 / Revised: 20 April 2024 / Accepted: 6 May 2024 /
Published online: 25 May 2024

Abstract

The present research work reported in air synthesis of a three-dimensional polymeric network of hydrogels by grafted copolymerization technique of Moringa gum and carboxymethyl cellulose by using acrylamide as a monomer, N, N-methylenebisacrylamide and ammonium persulphate as a cross-linker-initiator system. Different reaction parameters were used to optimize the synthesized hydrogel such as backbone ratio, pH of the reaction, temperature, volume of solvent, concentration of initiator, monomer and cross-linker with respect to the percentage swelling. The maximum percentage swelling 1244% was found at volume of solvent (17 mL), backbone ratio (2:1), cross-linker concentration (0.000032 $molL^{-1}$) and temperature (60 °C) and concentration of monomer (0.000042 $molL^{-1}$), and pH of 7. Mechanical strength and antibacterial properties of synthesized polymer networks are also evaluated. The confirmation of the synthesized hydrogel has been accomplished by using FTIR, FESEM, EDX, XRD, TGA and DSC characterization techniques. The synthesized hydrogels were evaluated as drug delivery carriers for in vitro release of antibiotic drug amoxicillin at pH of 2, 7 and 7.4. The drug release was compared between polymer matrices loaded with drug only and the polymer matrices loaded with Inclusion complex of β-Cyclodextrin and Amoxicillin. The controlled drug release has been found that is 99.25 ppm in 24 h in inclusion complex loaded polymer matrices, while the 75.472 ppm drug is released in just 8 h in the polymer matrices loaded directly with the drug. The Peppas-Sahlin equation holds good for release of amoxicillin at pH of 2 and 7, which further confirmed the diffusion and relaxation of polymer matrix are accountable the release of amoxicillin.

Extended author information available on the last page of the article

Graphical abstract

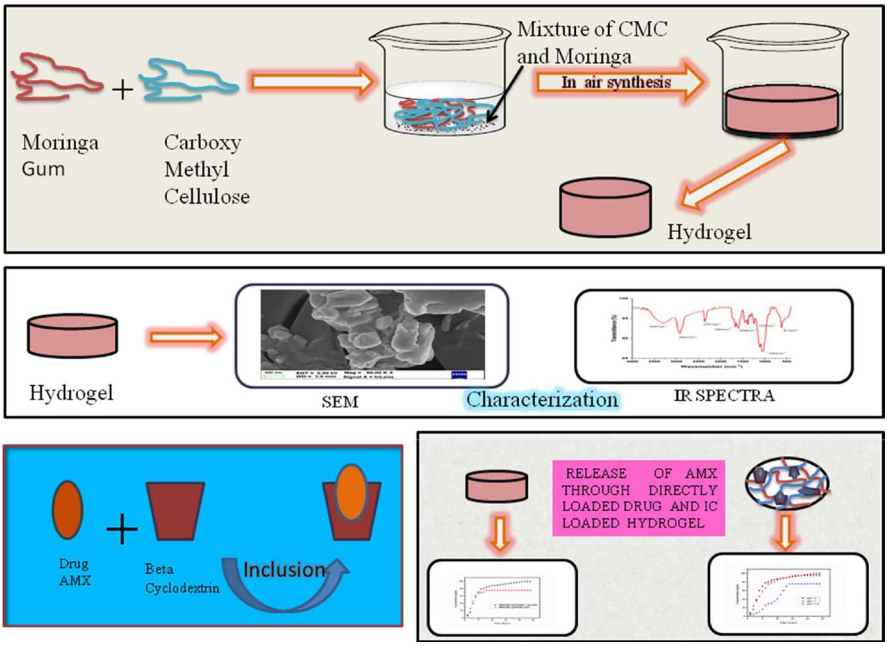

Keywords Moringa gum · Carboxymethyl cellulose · Controlled drug delivery · Inclusion complexes · Peppas-Sahlin

Introduction

Hydrogels have been extensively explored for their potential in drug delivery systems [1], tissue engineering, wound healing, biosensors and many other areas [2]. Their ability to capture and release therapeutic agents in a controlled manner makes them ideal candidates for drug delivery applications [3]. Hydrogels can be designed to respond to definite stimuli, such as pH, light, temperature, or electrical signals allowing for precise modulation of drug release kinetics. This unique property enables targeted and controlled delivery of drugs, minimizing side effects and improving therapeutic outcomes [4, 5]. Numerous drug delivery devices have been used for targeted drug delivery in the last decades. A few of them are polymeric hydrogel material [6–8], polypeptides, polymeric nanoparticles [9], gold nanoparticles [10], silica [11, 12], nanocomposites [13], and nanogels [14]. Among all drug delivery devices, the stimuli-responsive hydrogel networks as drug carriers have fascinated researchers. The pH-responsive drug delivery systems have the ability to release the drug molecules selectively at the desired pH range area. From the last decade, a large number of pH-responsive hydrogel materials have been used as drug carriers for site-specific drug delivery as they possess the desired properties

like biocompatible, biodegradable, cheap, and non-hazardous and can exhibit better acquiescence with the body of organism [15–17]. Among all drug delivery carriers, polysaccharide-based drug delivery systems have emerged as the most reliable carriers for the drug [18–22]. Various studies have been reported in the literature, where the polysaccharide-based hydrogel materials have been utilized as drug delivery systems like chitin, chitosan, carboxymethyl cellulose, pullulan, xanthan gum, dextrin and many more [21, 23–25].

Moringa Oleifera is a wild plant found in numerous tropical and subtropical countries. The Moringa Oleifera tree's stem produces a gum referred to as Moringa Oleifera gum (MOG), which starts off as white but modifies to brownish-black colour on exposure. When immersed in water, it forms a very sticky solution [26]. The composition of MOG includes D-galactose, D-mannose, and D-glucuronic acid, D-xylose, L-arabinose and L-rhamnose. It offers various health benefits, containing minerals, nutrients and a range of antioxidants. In India, MOG is commonly known as Sajna gum [27]. MOG and its derivatives exhibited enormous applications in various fields, including drug delivery, wastewater treatment, and as a pharmaceutical excipient [28–31]. In drug delivery applications, Singh and Kumar has synthesized dietary fibre Moringa gum-based hydrogels by grafting the polyvinyl pyrrolidine and evaluated the synthesized hydrogels for the release of the antibiotic drug meropenem [29]. Moringa gum and Sterculia gums were used to synthesize hydrogels by grafting polyacrylamide by the same research group and evaluate the same wound dressings by incorporating antibiotic drug levofloxacin. Moringa and polyacrylic-based hydrogels were also synthesized and utilized for the release of antibiotic levofloxacin [26]. The wound healing properties of moringa gum attracts scientists to utilize it in the synthesis of various formulations for drug delivery. MOG was exploited to form hydrogels by grafting (2-methacryloyloxy) ethyl trimethylammonium chloride and evaluated for ofloxacin release for wound healing [32]. Therefore, the literature available on MOG-based hydrogels, confirmed the utilization of MOG hydrogels as a drug release carrier in traditional drug delivery only. Carboxymethyl cellulose (CMC) is anionic and water-soluble derivative of cellulose and has various applications in dermal tissue engineering, drug delivery, protein delivery, scaffolds, artificial organs, wastewater treatment, cosmetics, plastics, paper industry [24, 33, and 34]. Because of its tuneable physical properties and polyelectrolytic nature, it has been utilized as an outstanding superabsorbent. Its biocompatibility, high stability, biodegradable properties, and binding capacity against pharmaceutically active compounds like enzymes and drugs make it a suitable candidate for drug delivery [24, 35, and 36]. Over the last few years, hydrogel materials of CMC have been explored for the delivery of a variety of drugs, including antibiotics, and anti-inflammatory and anticancer drugs agents [24, 35, 37–39]. Chemical cross-linking or blending of the biopolymers like CMC with other polymers either synthetic or natural improves the properties like chemical stability and mechanical strength [34]. Therefore, in this research work, CMC and MOG were selected as backbones and blended. In the present study, an attempt has been made to explore hydrogel materials synthesized from CMC and MOG by grafting the polyacrylamide chain for the drug release studies of antibiotic Amoxicillin (AMX). To the best of my knowledge, no work has been reported on the MOG/CMC-based cross-linked hydrogel

networks by incorporating preformed inclusion complexes of β-Cyclodextrin (β-CD) and AMX drug. There are some drawbacks associated with traditional drug delivery, including less drug loading capacity and less control over the mechanism of drug release. However, to overcome these issues, CMC and MOG-based hydrogel material was synthesized and was assessed as a carrier for AMX drug for controlled drug delivery. Therefore, the novelty also lies in the drug release studies from inclusion-loaded AMX were compared with the traditional drug delivery of AMX through the synthesized polymer matrices. Thus, the current effort highlights the synthesis and utilization of MOG and CMC-based hydrogel materials, as an efficient and promising candidate for the controlled drug delivery of AMX.

Materials and methods

Materials

Carboxymethyl cellulose sodium salt with medium viscosity (400–800 cps) was brought from HiMedia, India. Acrylamide, Ammonium persulphate and N–N' methylene bisacrylamide were purchased from HiMedia Laboratories Pvt. Ltd., Mumbai, India. Moringa Oleifera gum was collected from Srinagar, Uttarakhand, India. All the chemicals procured were used as such without any further purification.

Methods for preparation of hydrogel

In air synthesis of CMC and MOG-based hydrogel networks

The hydrogel has been synthesized using CMC and MOG as backbones and acrylamide as a monomer. Hydrogel was prepared by dissolving 0.40 g of CMC in distilled water. Further, 0.20 g MOG was added to the reaction mixture with constant stirring. The reaction mixture was mixed continuously till the formation of a uniform mixture. For the initiation of the reaction, initiator APS of 0.000219 $molL^{-1}$ was added. The addition of acrylamide (0.00042 $molL^{-1}$) was followed by the cross-linker MBA (0.00032 $molL^{-1}$) and the reaction mixture was mixed thoroughly to homogenize. The reaction mixture was placed at 60 °C in a hot air oven for the completion of the reaction. After the formation of hydrogel, washed with ethanol to remove unreacted materials and drying of hydrogel was done at 40 °C. The optimization of various reaction parameters such as initiator concentration ($molL^{-1}$), cross-linker concentration ($molL^{-1}$), time taken to complete the reaction (hrs), the volume of solvent (mL), temperature (°C), monomer concentration ($molL^{-1}$), and pH was varied to maximize the fluid uptake capacity or percentage swelling. The hydrogel networks are synthesized with or without incorporating inclusion complexes of β-CD with the drug Amoxicillin.

Microwave method (MW) for the preparation of inclusion complex (IC)

The preformed inclusion complexes of AMX and β-CD by microwave method were taken, the work already published by our research group [40]. In brief, the β-CD (1.314 g) was dissolved in distilled water at 45 °C and the AMX (0.419 g) was dissolved in ethanol. A molar ratio of 1:1 was taken for AMX and β-CD. The reactants are transferred to the microwave for the completion of the reaction. It takes 90 s. The precipitated form of ICs of AMX and β-CD were filtered. The product obtained was washed with ethanol to discard unreacted material. The powdered form of the product was kept in a vacuum oven to dry and stored for further studies.

Characterization of MOG/CMC-g-PAAM (IA) hydrogels

Numerous characterization techniques like FTIR, XRD, FESEM and EDS were utilized to characterize the synthesized sample and backbones used. The FTIR spectra of MOG, CMC, and MOG/CMC based Hydrogel networks, with a scanning range of $4000-400\ cm^{-1}$ on Perkin Elmer spectrophotometer using KBr pellets. UV–VIS analysis of AMX release from hydrogel matrices was accomplished on a systronics double beam UV–VIS Spectrophotometer (2201). Powder X-ray diffraction patterns of the samples were taken by scanning from 5 to 80° at a rate of 2° per minute to produce a diffraction pattern of MOG, CMC, and MOG/CMC by using panalytical X'Pert Pro multipurpose diffraction (MPD) with Cu-Kα radiation of wavelength 1.54 A^o at 298 K. Energy-dispersive spectroscopy (EDS) and field emission scanning electronic microscopy (FESEM) techniques were used to confirm the elemental composition and morphology of the surface of samples (MOG, CMC, and MOG/CMC based hydrogels) under various magnifications on SIGMA 500VP field emission scanning electron microscope with EDS and EBSD sensors. The thermal studies of the synthesized samples and all the backbone was carried out using a SII EXSTAR 6000 TGA/DTA/DTG thermal analyser in an inert atmosphere at a heating rate of 10 °C/ min within temperature range of 30–750 °C.

Swelling percentage studies

To evaluate the swelling characteristics of the synthesized hydrogel network, the dried and pre-weighed sample of hydrogel was put in 100 mL distilled water at room temperature. After a regular interval of time, the hydrogel was taken out and surface adhered water was removed by using filter paper. The dried sample was weighed. After attaining the equilibrium, the percentage swelling of the synthesized polymer networks was calculated by using equation one.

$$\%\text{Swelling} = \frac{W_s - W_d}{W_d} \times 100, \tag{1}$$

where W_s and W_d are the weight of swollen and dry polymer respectively.

Antibacterial studies

An antibacterial analysis was performed to validate the use of synthesized MOG/CMC-g-PAAM (IA) hydrogel matrices as drug delivery devices. Antibacterial characteristics of the hydrogel were performed by using the Agar well diffusion method [41] against the two strains of bacteria, Staphylococcus aureus and Escherichia coli.

Mechanical properties

Max stress (Pa) and percentage elongation at break (%E) of the MOG/CMC-based hydrogels without grafting and MOG/CMC-g-PAAM (IA) were tested in a universal testing machine (Lloyd Instruments) at a crosshead speed of 20 mm/min at 25 °C. ASTM D638 method was utilized to find the Max stress. The tensile stress was applied until the failure of the sample.

Drug delivery studies

In vitro drug release studies

The known concentrations of AMX solutions were prepared and the absorbance was determined at 217.0 nm on a UV–visible spectrophotometer. The standardization curve was plotted for the same. A pre-weighed sample of hydrogel (the Inclusion complex carrying hydrogel matrix or the directly loaded drug into the hydrogel matrix) was taken and immersed in 100 mL of releasing medium of different pH (2, 7 and 7.4) at 37 °C. After one hour, the 5 mL of sample is withdrawn and the concertation is measured concerning the standardization curve. The readings were noted down until the equilibrium was attained.

Release kinetics of AMX

It is quite difficult to predict the true mechanism of the release of drugs from a swelled hydrogel matrix. Water uptake capacity, diffusion, erosion of polymer matrix and relaxation are the different factors to govern the drug release studies. The drug release kinetics is studied by exploring four different models already stated in the literature [42–44]. These models are shown in the equations from 2 to 5.

Higuchi equation [45]

$$M_t / M_\infty = k.t^{0.5} \tag{2}$$

Here, Eq. 2, represents the Higuchi equation. Here, the fraction of the drug released (M_t/M_∞) is plotted against release time ($t^{0.5}$). This equation explains about Fickian diffusion.

Ritger–Peppas equation [46]

Equation 3, represents the Ritger-Peppas equation. In this equation, M_t/M_∞ is plotted against t^n. In this 'n', represents the diffusion exponent and it helped to determine the mechanism of the drug (AMX) release. If the slope (n) from the plot was found to be 0.5, the normal Fickian diffusion will be accountable for the drug release. But, if 'n' was calculated between 0.5 and 1, the non-Fickian diffusion is responsible for the drug release. If the value of 'n' is equal to 1, the drug release was the case of case-II diffusion which corresponds to zero-order kinetics.

$$M_t/M_\infty = k.t^n \tag{3}$$

Zero-order equation [47]

Equation 4, represents the Zero-order kinetics. The graph is plotted between fraction of the drug release and time (t) and 'k' is a kinetic constant.

$$M_t/M_\infty = k.t \tag{4}$$

Peppas–Sahlin equation [48]

Equation 5, represents Peppas-Sahlin equation. The k_1 is diffusion constant and k_2 is relaxation constant. The values of 'm' are taken differently for the different shapes. In thin film samples, the value of m is taken as 0.5 and it has been taken as 0.5 for cylindrical hydrogel samples.

$$M_t/M_\infty = k_1.t^m + k_2.t^{2m} \tag{5}$$

Using the calculated values of k_1 and k_2 from Eq. 5, the ratio of relaxation (R) to Fickian (F) contributions was estimated [49] using Eq. 6 as

$$R/F = \left(k_2/k_1\right)t^m \tag{6}$$

Results and discussions

Optimization parameters (Effect of different parameters on percentage swelling)

Temperature: Temperature has a remarkable effect on the percentage swelling of the hydrogel. The temperature range was kept from 40° to 80 °C. The swelling percentage was found maximum at 60 °C (Fig. 1a). The percentage swelling was enhanced with the

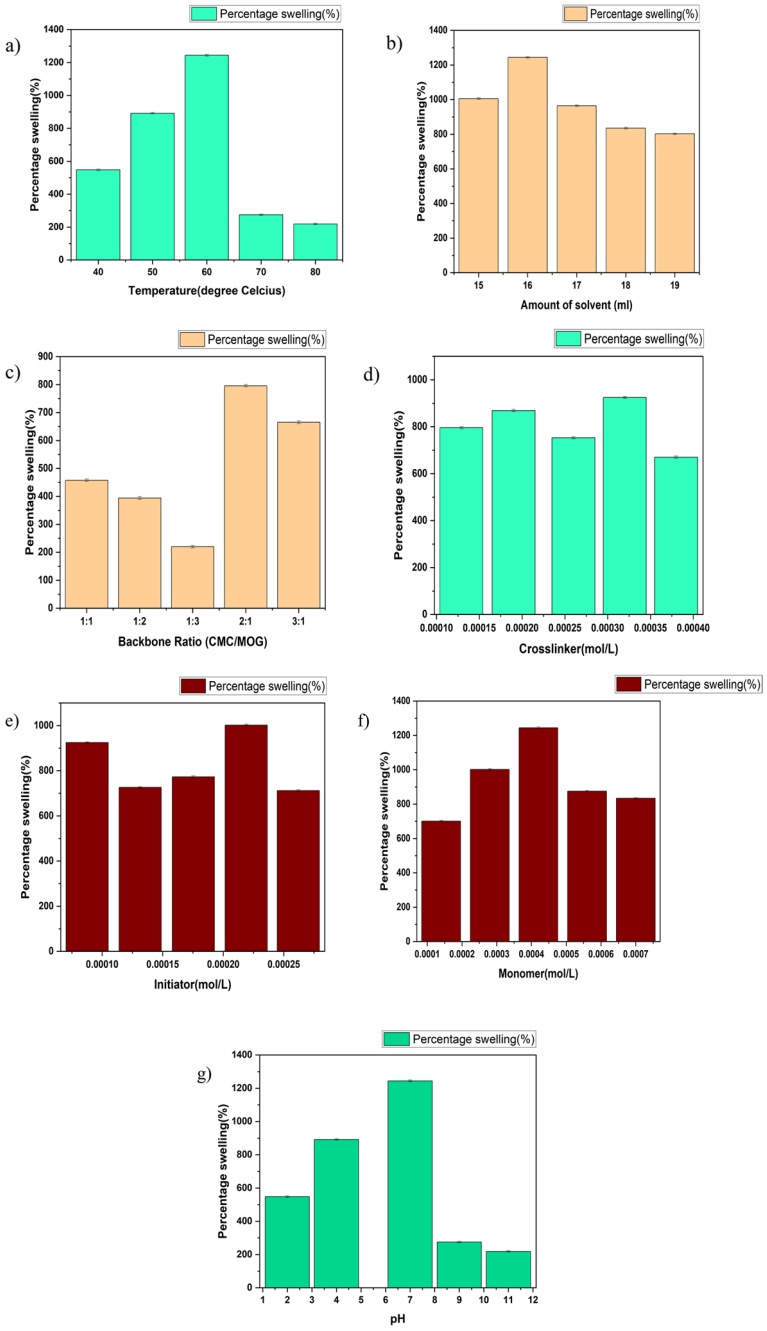

Fig. 1 Optimization graphs for the synthesis of MOG/CMC-g-PAAM (IA) hydrogels (**a**) Temperature, (**b**) Solvent, (**c**) Backbone ratio, (**d**) Concentration of cross-linker, (**e**) Concentration of Initiator (**f**) Concentration of monomer

increase in temperature initially and after reaching the maximum value it decreased, this might be due to the over-crosslinking of the polymeric chains at the higher temperature leads to the denser network which leads to lesser water uptake capacity.

Volume of the solvent: The volume of solvent is varied from 15 to 19 mL (15, 16, 17, 18, and 19 mL) and the percentage of swelling was studied. With the increase in the amount of solvent, the percentage swelling increases (Fig. 1b) to a certain extent due to a diffusion-controlled phenomenon, after which it decreases upon further increasing the amount of solvent [50]. The solvent provides a medium for interactions of different functional groups but after an optimal value, the percentage swelling decreases might be due to the movement of more ions into the medium that can interact with the cross-linking density of the polymer matrix. Therefore, the most optimized volume of solvent was 16 mL and swelling were 1244%.

Backbone Ratio: The backbone ratio (CMC: MOG) plays a crucial role in deciding the fluid uptake capacity of the synthesized hydrogel material. The amount of CMC and MOG taken is varied from 1:1, 2:1, 3:1, and 1:2. 1:3. The maximum percentage swelling of the synthesized hydrogel material was 2: 1 (Fig. 1c), therefore, the most optimized ratio was observed as 2:1 (CMC: MOG). This might be due to an increase in hydrophilicity of the polymer matrix at 2:1 which results in appropriate electrostatic and hydrogen bonding interactions among the polymeric chains in the polymeric matrix. But on further increasing the ratio to 3:1, the percentage swelling decreases might be due to the extra functional sites present in the polymeric matrix resulting in lesser effective interactions and poor hydrogen bonding.

The Concentration of cross-linker: The percentage swelling was increased upon increasing the concentration of MBA initially might be due to the synthesis of porous structure which enabled more liquid uptake into the polymer matrix. The most optimized concentration of MBA is 0.000032 $molL^{-1}$ (Fig. 1d). On further increasing the concentration of MBA, the percentage swelling decreases might be out to the more crosslinking may lead to the compact structure of the polymer network which cannot accommodate the more liquid molecules inside the polymer matrix [29].

The Concentration of monomer: The effect of monomer concentration was studied at the preoptimized condition of the volume of solvent (17 mL), backbone ratio (2:1), cross-linker concentration (0.000032 $molL^{-1}$) and temperature (60 °C). The most optimized concentration of AAM is 0.000042 $molL^{-1}$ (Fig. 1e). Further increase in monomer concentration results in the decline in the percentage swelling, which might be due to the higher concentration of monomer may result in more grafting which ultimately leads to more cross-linking density and provides less room to incoming water molecules into the polymer matrix.

The Concentration of initiator: The effect of the initiator was studied on preoptimized conditions volume of solvent (17 mL), backbone ratio (2:1), cross-linker concentration (0.000032 $molL^{-1}$) and temperature (60 °C) and concentration of

monomer (0.000042 molL^{-1}). The most optimized concentration of APS was found 0.000219 molL^{-1} as shown in Fig. 1f.

pH: The swelling studies have been performed at different pH ranges (2 to 11). The synthesized hydrogel exhibited the maximum percentage swelling at neutral pH (Fig. 1h) and was found to be pH-responsive. The percentage swelling was less at a pH of 2, which might be due to more electrostatic repulsion in the acidic medium as the hydrogel gets protonated. As pH increases, the percentage swelling increases and found maximum at neutral pH might be due to the deprotonation of functional groups present in polymer matrix leading to more hydrogen bonding among polymeric chains which can accommodate more water inside it around hydrogen-bonded groups and capillary pores, resulting in maximum swelling. At basic pH, deprotonation of functional groups leads to a decrease in the degree of ionization which leads to the formation of a compact structure owing to the extensive hydrogen bonding which results in a lesser percentage swelling [51].

Proposed reaction mechanism for hydrogel formation

The synthesis of MOG/CMC-g-PAAM (IA) hydrogel network has been synthesized by free radical polymerization mechanism. The physical appearance of MOG, CMC and synthesized hydrogel is given in Fig. 2. The APS first generates a free radical anion of sulphate by thermal decomposition as shown in step I, which further reacts with water to generate hydroxyl free radical. The hydroxy free radicals further generate active sites or free radicals on CMC and MOG. The free radicals further attack the double bond of acrylamide and generate free radicals which copolymerized to form a long chain and the chain is propagated by grafting on polymeric chains. Further, the cross-linker, MBA also generates the free radicals and cross-linked the different polymeric chains as shown below in the mechanism.

Fig. 2 Physical appearance of CMC, Moringa Gum and MOG/CMC-g-PAAM (IA) hydrogel

Step I:

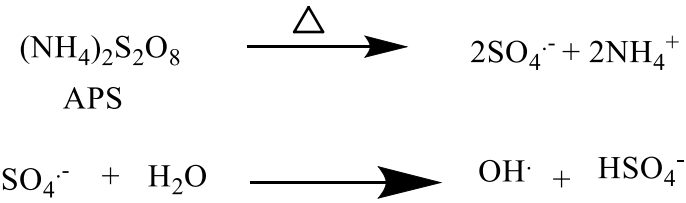

Step II:

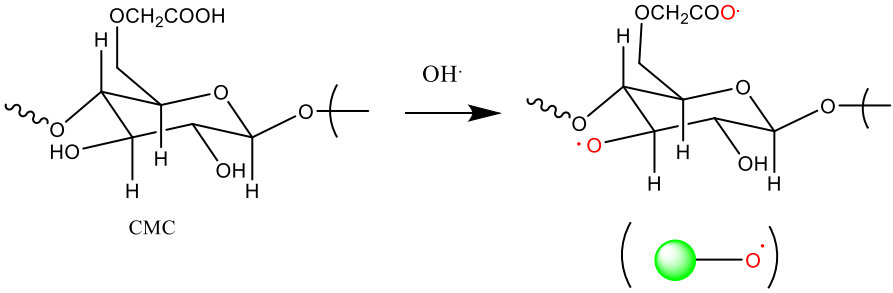

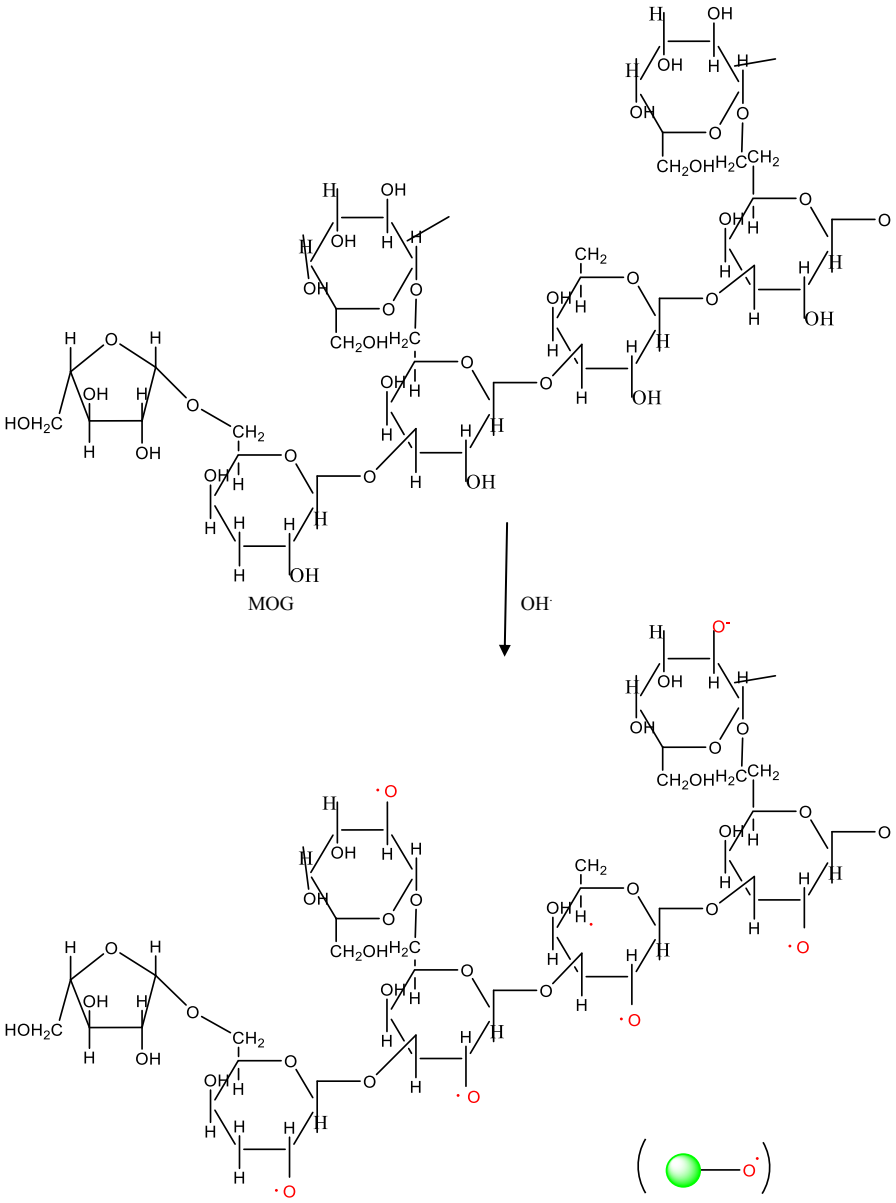
MOG
OH-

Step III:

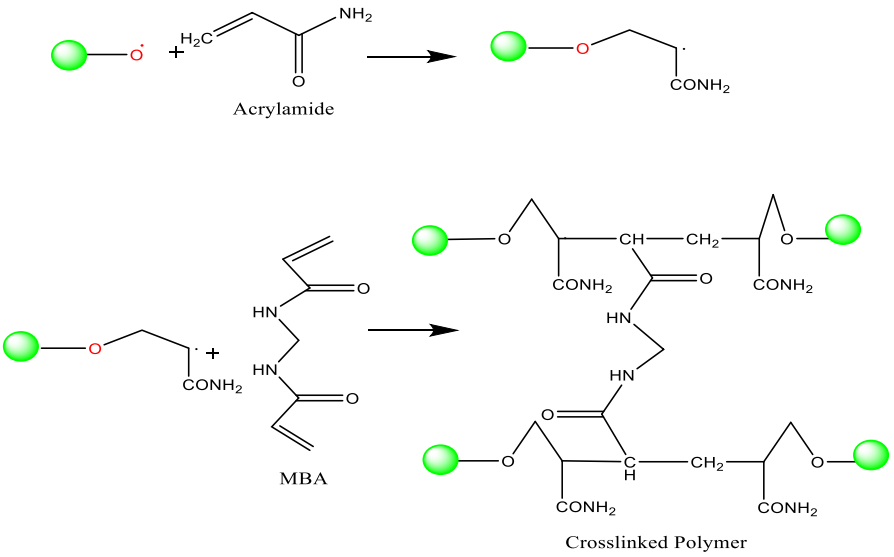

Characterization

Fourier transform-infrared spectroscopy

In the FT-IR of CMC (Fig. 3a), there are characteristic peaks at 1600 cm^{-1} for the carbonyl group of acid [35], 2920 cm^{-1} for C-H stretch of methylene, 1041 cm^{-1} for C–O–C (ether), 1409 cm^{-1} for deformations in methylene and a broad band was observed at 3282 cm^{-1} for the presence of –OH groups [39]. In FT-IR of Moringa Oleifera gum (Fig. 3b), the absorption peak at 3390 cm^{-1} represents the C-H stretch of alkynes, whereas alkanes are represented by the peak at 2927 cm^{-1}. The peak at 1713 cm^{-1} represents the C=O stretch of ester, whereas the O=C–O–C stretch at 1244 cm^{-1} represents another class of ester. By considering the FT-IR of most optimized hydrogel, it is seen that the peak at 1600 cm^{-1} is absent, which indicates at removal of the C=C bond. Also=C-H Stretching at 3000 cm^{-1} is absent (Fig. 3c). The absence of these two peaks confirms that acrylamide is grafted on the polymeric chain.

X-Ray diffraction studies

X-ray diffraction studies are utilized as one of the significant tools to witness hydrogel formation. The diffraction profile of CMC (Fig. 4a) is almost amorphous with crystalline three sharp peaks [34]. The broad large peaks present in the XRD of MOG (Fig. 4b) confirmed the amorphous nature of MOG. The inoculation of three

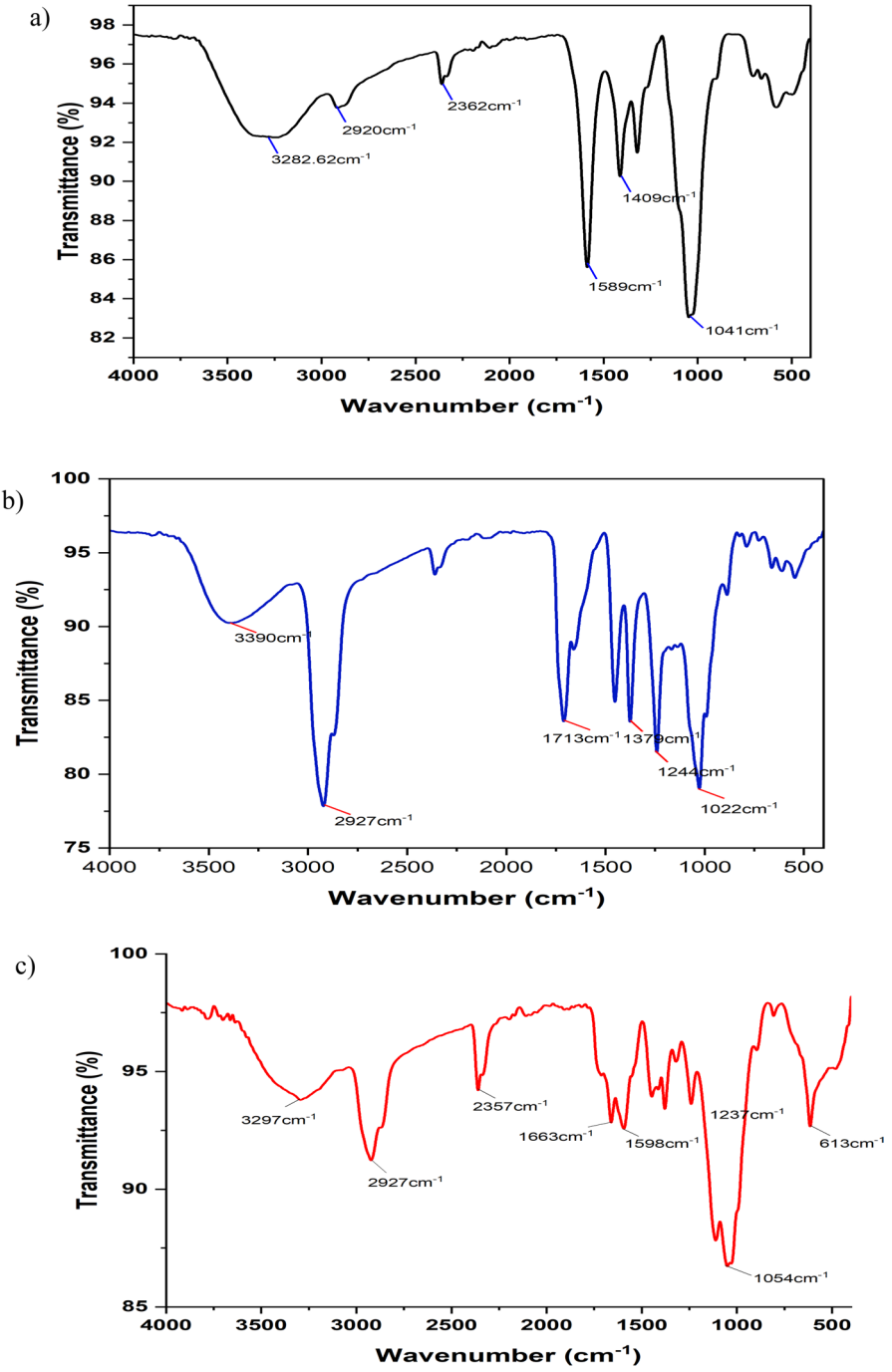

Fig. 3 FTIR Spectra of (**a**) CMC (**b**) MOG (**c**) MOG/CMC-g-PAAM (IA) Hydrogels

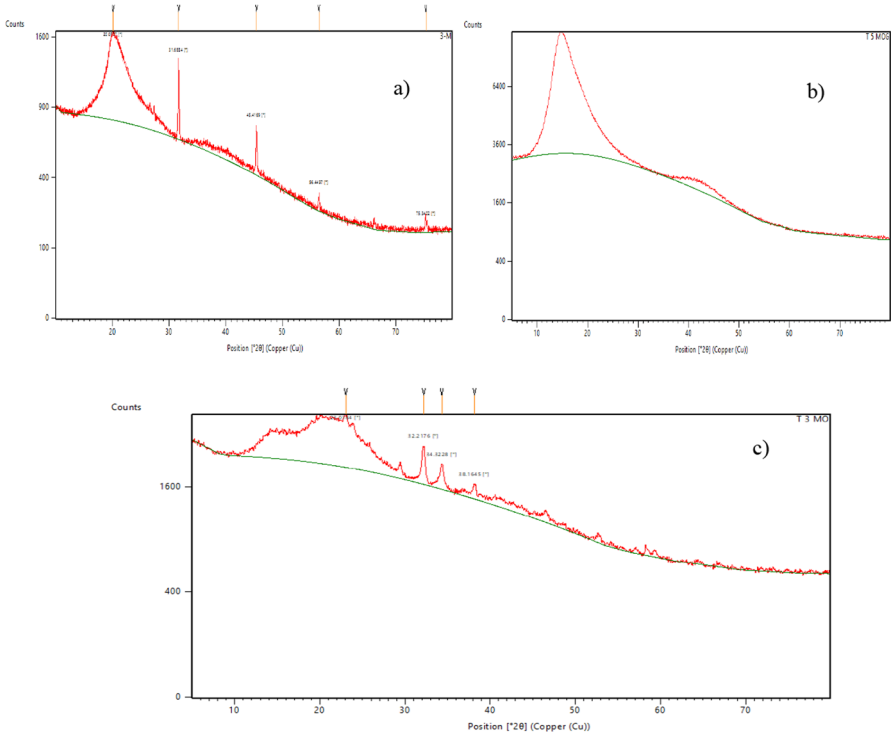

Fig. 4 XRD Spectra of **a** CMC **b** MOG **c** MOG/CMC-g-PAAM (IA) Hydrogels

sharp peaks of CMC and the broad peak of MOG in the diffraction pattern of hydrogel (Fig. 4c) confirmed the formation of hydrogel from Moringa gum and CMC.

Field-emission scanning electron microscopy (FESEM)

The FESEM images of the CMC, moringa gum and MOG/CMC-g-polyacrylamide Hydrogel have been shown in Fig. 4. From the FESEM data, it is clear that CMC has a rough surface (Fig. 5a). The surface of Moringa gum (Fig. 5b) is also rough. But on grafting the acrylamide on the polymeric chains of moringa gum and CMC, the surface becomes more porous, rough, and heterogeneous as can be seen in the FESEM image of the synthesized hydrogel (Fig. 5c).

EDS studies

The EDS spectrum of CMC (Fig. 5d) confirmed the presence of Na, C and O. The EDS spectrum of Moringa gum (Fig. 5e) confirmed the presence of C and O. The EDS spectrum of synthesized hydrogel network CMC/MOG-g- PAAM (Fig. 5f) has revealed the occurrence of all the elements present that is C, O, Na, and a very small peak of N in between C and O which confirmed the grafting of polyacrylamide on the chains of Moringa gum and CMC and cross-linking with MBA.

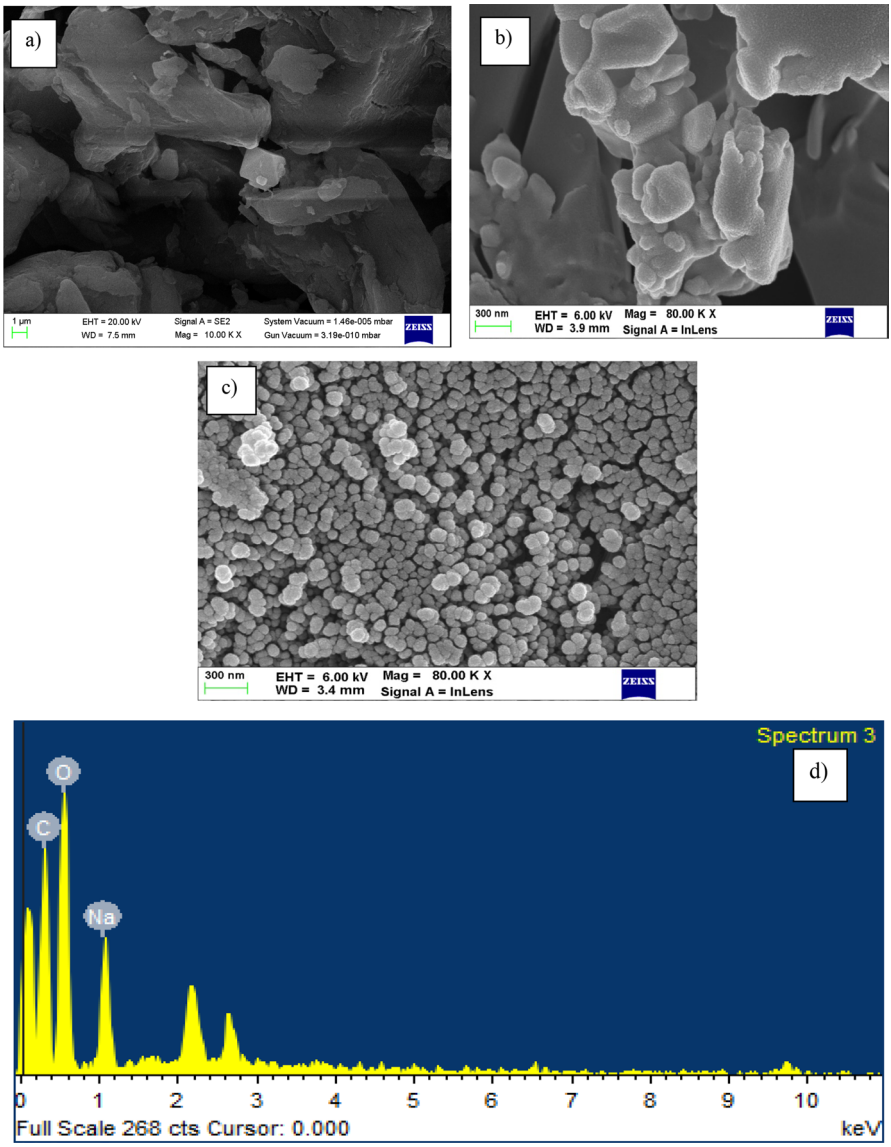

Fig. 5 FESEM Images of (**a**) CMC (**b**) MOG (**c**) MOG/CMC-g-PAAM (IA) Hydrogels. EDX Pattern of (**d**) CMC (**e**) MOG (**f**) MOG/CMC-g-PAAM (IA) Hydrogels

TGA studies

Figure 6a shows the percentage weight loss in MOG, CMC and CMC/MOG-g-PAAM (IA) as a function of temperature. It is clear from the TGA curve, MOG has expressed three-stage decomposition. The first stage of decomposition lies in the range of 50–130 °C with a weight loss of 15.57% due to the loss of moisture

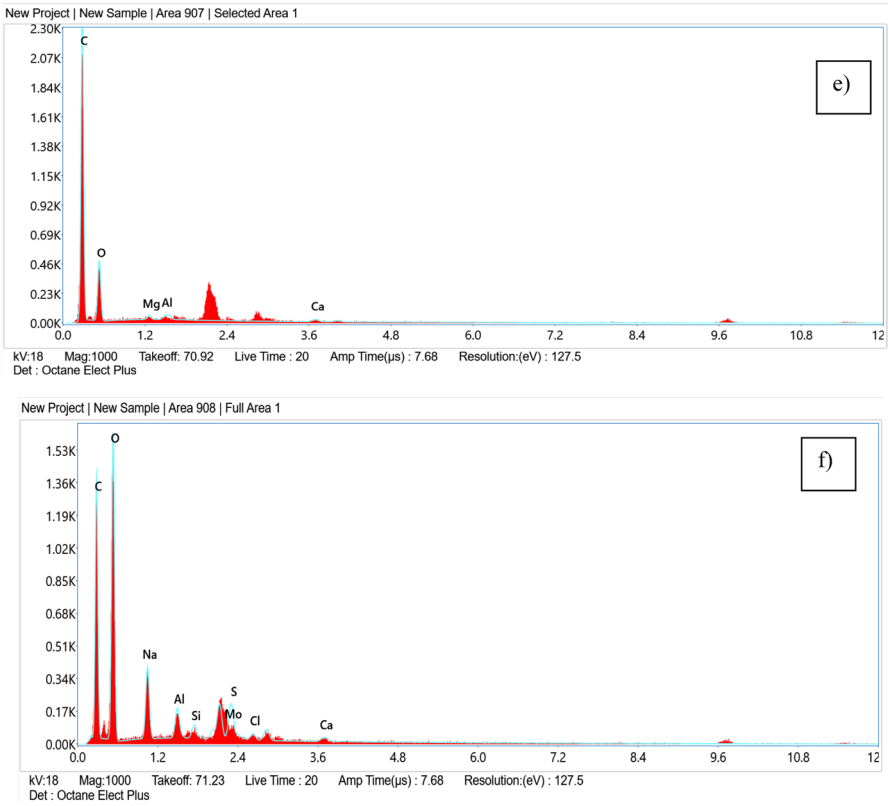

Fig. 5 (continued)

bound to the saccharide part of MOG and dehydration owing to the loss of hydroxyl groups present on the polysaccharide chain [52, 53]. The second stage of decomposition lies in the range of 139–301 °C with a weight loss of 38.37%. The final stage of decomposition ranged from 305 to 615 °C with a weight loss of 46%. This is attributed to the breakdown of the polymeric chain and pyrolytic decomposition with the loss of small molecules like CO, CO_2, and CH_4. MOG degraded completely around 615 °C. The GA curve of CMC has also shown the three-stage decomposition. The first stage lies from 50 to 105 °C with 10% weight loss, the second stage lies from 122 to 287 °C with 30% and the third stage lies from 305 to 661 °C with 56% weight loss. The final decomposition temperature of CMC was found to be 661 °C with a 96% weight loss. The TGA curve of CMC/MOG-g-PAAM (IA) has revealed the four-stage decomposition. The first stage of decomposition lies from 40 to 140 °C with a weight loss of 12%. The second stage lies from 147 to 238 °C with 28% weight loss, the third stage lies from 240 to 456 °C with 30% weight loss and the final stage lies from 460 to 771 °C with 39% degradation. The degradation rate slow down from 500

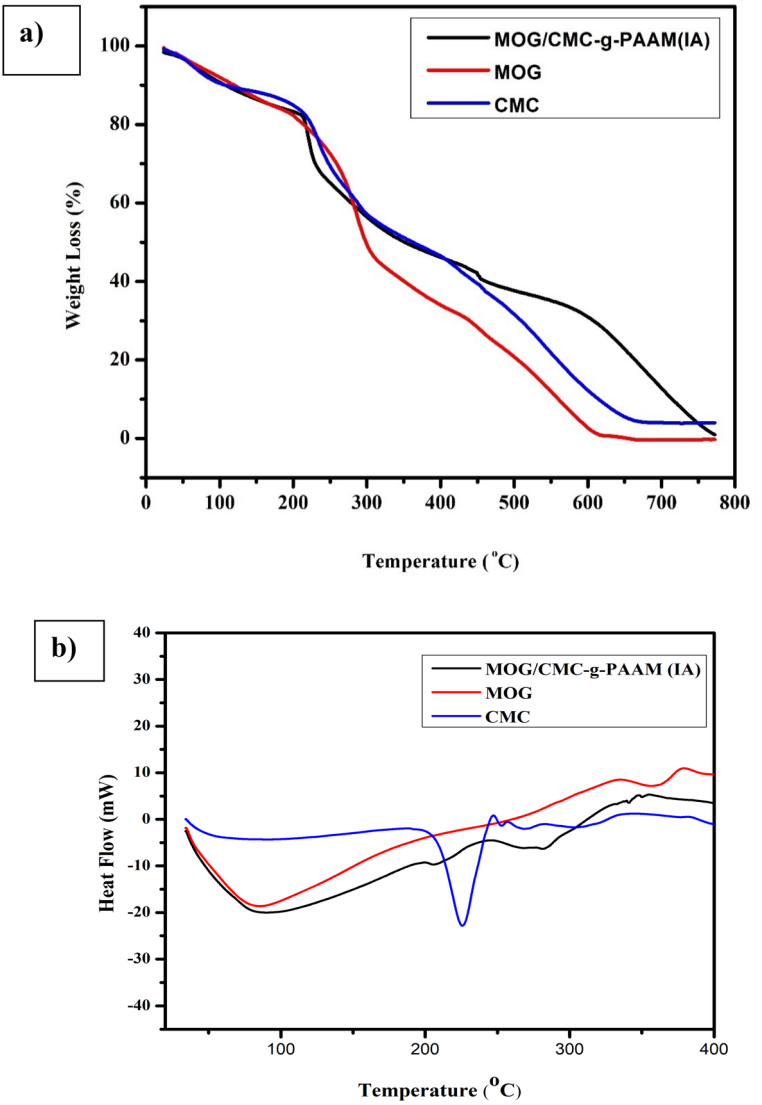

Fig. 6 **a** Thermal gravimetric analysis of CMC, MOG, and MOG/CMC-g-PAAM (IA) Hydrogel. **b** DSC analysis of CMC, MOG, and MOG/CMC-g-PAAM (IA) Hydrogel

to 600 °C with weight loss of only 6%. The final decomposition temperature of the synthesized polymer matrix was 771 °C with 99% weight loss which is higher than both the MOG (615 °C) and CMC (661 °C) from which it has been synthesized. The TGA studies confirmed the synthesized hydrogels were found to be thermally more stable due to the covalently bonded crosslinking among the polymeric chains of MOG, CMC and PAAM.

DSC studies

Thermal transitions of the backbones and synthesized polymer materials were analysed by using the DSC technique. Glass transition temperature is very important for amorphous and semicrystalline materials to decide their application in different fields. DSC results have been shown in Fig. 6b. DSC thermogram of MOG revealed a broad endothermic peak and two small exothermic peaks in accordance with the literature [54]. The glass transition endothermic peak was observed around 90 °C, which onsets around 35 °C and ends around 200 °C. The two exothermic peaks appeared at 333.67 and 378.4 °C. The DSC thermogram of CMC has shown its glass transition temperature (Tg) around 45 °C and an endothermic peak around 226 °C has revealed its melting point (Tm), therefore the presence of Tg and Tm both in the DSC thermograph of CMC confirmed ita semicrystalline nature and supports the results obtained from XRD. The DSC thermograph of the hydrogel has shown two broad endothermic peaks (one broad and the other small) and one small exothermic peak. The broad endothermic peak observed around 95 °C which onsets around 35 °C and ends around 245 °C and a small endothermic peak starts 246 °C and ends at 301 °C. The exothermic small and broad peak was observed around 350 °C.

Antibacterial studies

Figure S1 demonstrated the antibacterial results of the CMC/MOG-g-PAAM (IA) for gram-positive bacteria S. aureus and gram-negative bacteria E. coli. The antibacterial properties of the synthesized matrices were found might be due to the presence of MOG and CMC in the polymer matrices. The zone of inhibition was measured 18 mm for S. aureus and 13 mm for E. coli. The antibacterial analysis of the hydrogel matrices revealed its ability to combat bacterial infections. It confirmed the utilization of the synthesized hydrogels in the controlled release of AMX is innocuous.

Mechanical properties

The tensile strength of MOG/CMC hydrogels without grafting of polyacrylamide and MOG/CMC-g-PAAM (IA) hydrogels was found to be 7.25 ± 0.55 Pa (NM^{-2}) and 9.25 ± 0.35 Pa (NM^{-2}), respectively. The elongation at break was found to be $33.65 \pm 0.45\%$ and $37.8 \pm 0.5\%$ for MOG/CMC and MOG/CMC-g-PAAM (IA) hydrogels respectively. The results obtained are comparable to the mechanical properties of MOG-based hydrogels in the literature [28]. The increase in the tensile strength and elongation at break in the MOG/CMC-g-PAAM (IA) is might be due to grafting of the polyacrylamide chains onto the MOG and CMC that results in the enhancement in the roughness of the surface of the polymer matrix as compared to the un-grafted polymer matrix.

Release kinetics of AMX from the synthesized polymer matrix

Figure 7, establishes the AMX release patterns through the ICs-loaded polymer matrices and directly loaded polymer matrices with AMX containing CMC/MOG-g-PAAM (IA). The graph (Fig. 7a) shown the release of AMX through directly loaded matrices CMC/MOG-g-PAAM: AMX (IA) was burst type and the total (75.472 ppm) AMX release occurred in just 8 h at pH of 7. But the AMX loaded through inclusion complexes get released (90.25 ppm) CMC/MOG-g-PAAM-β-CD: AMX (IA) in 24 h which showed the controlled release. The reason for controlled release might be due to AMX release from the β-CD hollow void to the matrices of the polymer network followed by the release from matrices to the releasing medium. Figure 7b exhibited the release pattern of AMX through CMC/MOG-g-PAAM-β-CD: AMX (IA) at pH 2, 7, 7.4 and 37 °C. The release pattern at pH of 4.6 and 6.8 pH is also compared with the pH of 2, 7 and 7.4 in Fig. S2. Initially, the AMX release after 2 h interval was found (Fig. 7b) as 5.5 ppm, 23.77 ppm, and 4.55 ppm at pH of 2, 7 and 7.4 respectively. After 24 h, the total drug release was found to be 99.25 ppm, 95.45 ppm and 75.87 ppm at a pH of 2, 7 and 7.4 respectively. So, the descending order of AMX release was acidic medium > neutral > basic medium which was further confirmed from Fig. S2 too, which includes the drug release data performed at pH of 4.6 and 6.8 along with the pH of 2, 7 and 7.4. The kinetics were applied to the drug release data obtained at 2, 7 and 7.4. The value of diffusion exponent (Table 1 and Fig. 7c–e) was found to be 0.665, 0.701 and 1.154 at pH off 2, 7 and 7.4 CMC/MOG-g-PAAM-β-CD: AMX (IA). The value of diffusion exponent lies between 0.5 and 1, confirming the non-Fickian diffusion of AMX from the polymer matrix at pH of 2 and 7. The value of diffusion exponent was found to be 1.154 at pH of 7.4 confirming the super case II transport. The values of K_1 were found to be more than the K_2 values (negative) in the Peppas-Sahlin equation confirmed the diffusion suppresses the relaxation process in AMX release. The data fits well into the Peppas -Sahlin equation for the AMX release at pH of 2 and 7. But no equation out of these four holds good for the drug release at pH of 7.4. A graph is plotted between the ratio (R/F) fraction of AMX released (Fig. 7f). Thus, it revealed the order of the rate of relaxation among the polymeric chains at different pH values that is 7.4 > 2 > 7.

Table 1 Fitting of AMX release to diverse models through MOG/CMC-g-PAAM/βCD: AMX (IA) Hydrogels

pH	Higuchi		Ritger Peppas			Peppas Sahlin			Zero-order	
	$k\ (h^{-0.5})$	R^2	n	$k'\ (h^{-n})$	R^2	$k_1\ (h^{-0.5})$	$k_2\ (h^{-1})$	R^2	$k''\ (h^{-1})$	R^2
2	0.2024	0.780	0.665	−1.841	0.776	0.351	−0.03	0.989	0.0291	0.630
7	0.2199	0.840	0.701	−1.925	0.806	0.3290	−0.0224	0.990	0.0319	0.693
7.4	0.3178	0.915	1.154	−3.336	0.956	0.0639	0.0370	0.9738	0.0439	0.870

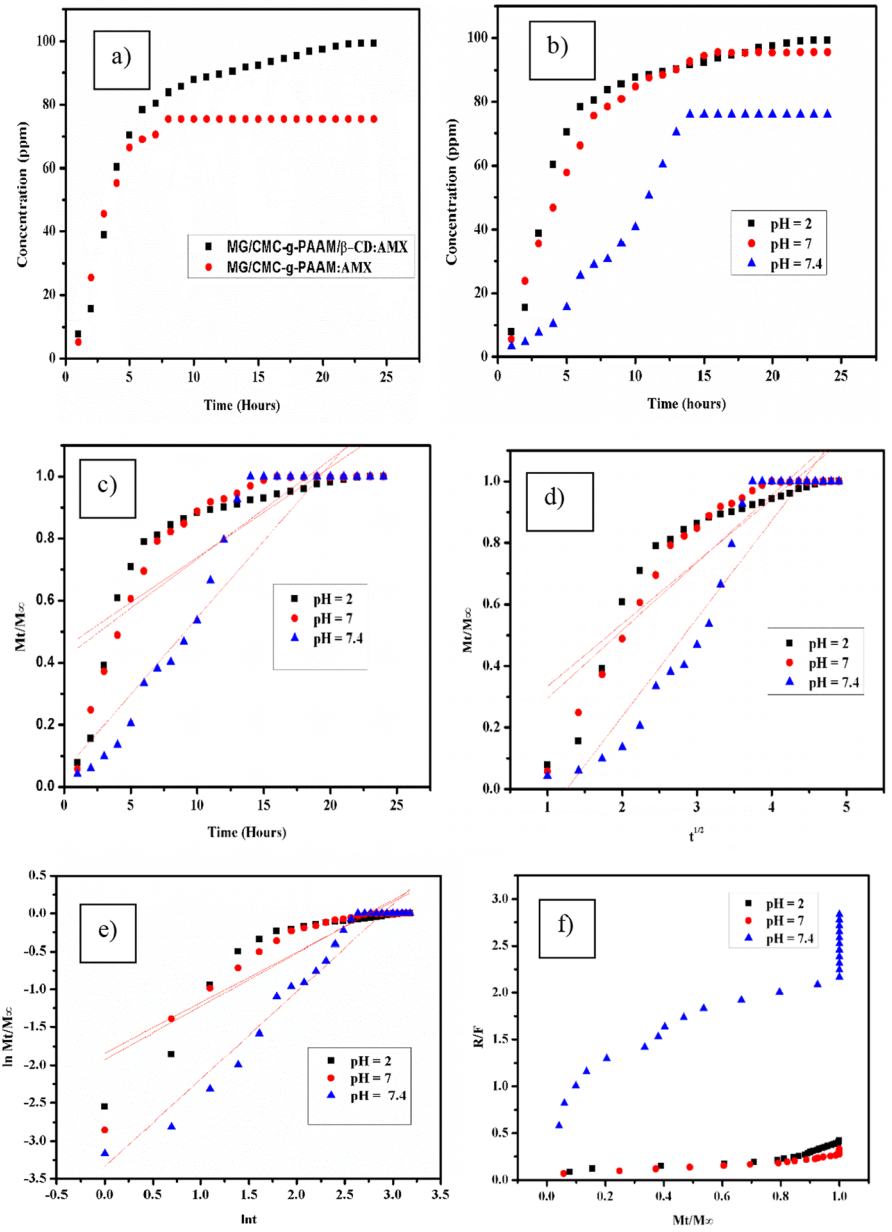

Fig. 7 Release kinetics of drug AMX through the polymer matrices MOG/CMC -g-PAAM (IA) and MOG/CMC -g-PAAM/βCD: AMX (IA) Hydrogels. (**a**) A plot between concentration and time for inclusion complexes loaded hydrogels and directly loaded AMX into Hydrogel matrix. (**b**) A plot between concentration and time for inclusion complexes loaded hydrogel matrices at different pH values. (**c**) A plot between fractional drug release ($Mt/M\infty$) and time at different pH values. (**d**) A plot between fractional drug release ($Mt/M\infty$) and $t1/2$ at different pH values. (**e**) A plot between fractional drug release ($Mt/M\infty$) and lnt at different pH values. (**f**) A plot between relaxation to Fickian ratio and fraction of drug release at different pH values

Conclusions

In the present research work, the hydrogel networks of MOG and CMC were successfully synthesized and optimized in air conditions. The most optimized hydrogel networks exhibited a percentage swelling of 1244% at pH of 7 and 60 °C temperature. The hydrogels were loaded with the ICs of the drug and evaluated for AMX release studies and compared with the directly loaded AMX in the polymer matrix. The AMX release was found to be highest in the acidic medium (99.25 ppm) followed by the neutral medium (95.45 ppm). It was found lowest in the basic medium (75.87 ppm). The release of AMX was found to be 75.472 ppm in just 8 h in directly loaded drugs at neutral pH but the drug release through the ICs of AMX and β-CD has revealed the controlled release of AMX (95.45 ppm) in 24 h. The drug release of AMX fits well with the Peppas -Sahlin equation at pH of 2 and 7. Therefore, the synthesized CMC/MOG-g-PAAM-β-CD: AMX (IA) hydrogel is an effective controlled drug delivery system to release the drug AMX in the pH range from acidic to neutral (2–7) medium.

Supplementary Information The online version contains supplementary material available at https://doi.org/10.1007/s00289-024-05304-y.

Acknowledgements The author is thankful to the central instrumentation facility, LPU and Institute Instrumentation Centre facility (IIC), DR B R Ambedkar National Institute of Technology, Jalandhar for the characterization of samples by using different techniques like FESEM, EDS, XRD and FTIR.

Author contribution Lakhveer Kaur: Visualization, Investigation, Writing—original draft. Anmol: Conceptualization and software handling. Mehak Sharma: Data Organization. Rajeev Jindal: Formal analysis, Kuljit Kaur: Data curation, Methodology, Validation, Writing—review & editing, Supervision.

Declarations

Conflict of interests The authors declare no competing interests.

References

1. Bajpai AK, Shukla SK, Bhanu S, Kankane S (2008) Responsive polymers in controlled drug delivery. Prog Polym Sci 33:1088–1118
2. Brahim S, Narinesingh D, Guiseppi-Elie A (2002) Bio-smart hydrogels: co-joined molecular recognition and signal transduction in biosensor fabrication and drug delivery. Biosens Bioelectron 17:973–981. https://doi.org/10.1016/S0956-5663(02)00089-1
3. Li J, Mooney DJ (2016) Designing hydrogels for controlled drug delivery. Nat Rev Mater 1:1–18. https://doi.org/10.1038/natrevmats.2016.71
4. Buwalda SJ, Vermonden T, Hennink WE (2017) Hydrogels for therapeutic delivery: current developments and future directions. Biomacromol 18:316–330. https://doi.org/10.1021/acs.biomac.6b01604
5. Das S, Subuddhi U (2016) Controlled and targeted delivery of diclofenac sodium to the intestine from pH-Responsive chitosan/poly(vinyl alcohol) interpenetrating polymeric network hydrogels. Polym Sci Ser A 58:154–166. https://doi.org/10.1134/S0965545X16020048

6. Mittal H, Mishra SB, Mishra AK et al (2013) Flocculation characteristics and biodegradation studies of Gum ghatti based hydrogels. Int J Biol Macromol 58:37–46. https://doi.org/10.1016/j.ijbiomac.2013.03.045
7. Kaur K, Jindal R, Tanwar R (2019) Chitosan-gelatin @ tin (IV) tungstatophosphate nanocomposite ion exchanger: synthesis, characterization and applications in environmental remediation. J Polym Environ 27:19–36. https://doi.org/10.1007/s10924-018-1321-5
8. Sharma P, Jindal R (2018) Gum Dammar and poly(acrylamide)-based hydrogels and zirconium-based organic-inorganic hybrid materials for controlled drug delivery and their biodegradation studies. Polym Bull 75:4175–4190. https://doi.org/10.1007/s00289-017-2261-2
9. Agboola O, Fayomi OSI, Ayodeji A et al (2021) A review on polymer nanocomposites and their effective applications in membranes and adsorbents for water treatment and gas separation. Membranes (Basel) 11:1–33
10. Baei P, Jalili-Firoozinezhad S, Rajabi-Zeleti S et al (2016) Electrically conductive gold nanoparticle-chitosan thermosensitive hydrogels for cardiac tissue engineering. Mater Sci Eng C 63:131–141. https://doi.org/10.1016/j.msec.2016.02.056
11. Kaur K, Jindal R, Bandhu M (2020) Monodispersed silica nanoparticles incorporated nanocomposites of gelatin and psyllium for sequestration of noxious pollutants. J Polym Environ 28. https://doi.org/10.1007/s10924-019-01591-z
12. Ma B, He L, You Y et al (2018) Controlled synthesis and size effects of multifunctional mesoporous silica nanosystem for precise cancer therapy. Drug Deliv 25:293–306. https://doi.org/10.1080/10717544.2018.1425779
13. Priya KBS, Shanker U et al (2018) RSM-CCD optimized In-air synthesis of photocatalytic nanocomposite: application in removal-degradation of toxic brilliant blue. React Funct Polym 131:107–122. https://doi.org/10.1016/j.reactfunctpolym.2018.07.016
14. Jiang Y, Chen J, Deng C et al (2014) Click hydrogels, microgels and nanogels: emerging platforms for drug delivery and tissue engineering. Biomaterials 35:4969–4985
15. He M, Chu CC (2013) Dual stimuli responsive glycidyl methacrylate chitosan-quaternary ammonium hybrid hydrogel and its bovine serum albumin release. J Appl Polym Sci 130:3736–3745. https://doi.org/10.1002/app.39635
16. Sukriti SJ, Pruthi V et al (2016) Surface response methodology-central composite design screening for the fabrication of a Gx-psy-: G -polyacrylicacid adsorbent and sequestration of auramine-O dye from a textile effluent. RSC Adv 6:74300–74313. https://doi.org/10.1039/c6ra12715k
17. De Yao K, Xuan XuM, Ji Yin Y et al (1996) pH-Sensitive chitosan/gelatin hybrid-polymer network microspheres for delivery of cimetidine. Polym Int 39(4):333–337
18. Mittal A, Garg S, Kohli D et al (2016) Effect of cross linking of PVA/starch and reinforcement of modified barley husk on the properties of composite films. Carbohydr Polym 151:926–938. https://doi.org/10.1016/j.carbpol.2016.06.037
19. Xu YX, Kim KM, Hanna MA, Nag D (2005) Chitosan-starch composite film: preparation and characterization. Ind Crops Prod 21:185–192. https://doi.org/10.1016/j.indcrop.2004.03.002
20. European Medicines Agency E (2014) Background review for cyclodextrins used as excipients
21. Sharma J, Sukriti AP et al (2017) RSM-CCD optimized adsorbent for the sequestration of carcinogenic rhodamine-B: kinetics and equilibrium studies. Mater Chem Phys 196:270–283. https://doi.org/10.1016/j.matchemphys.2017.04.042
22. Kumari P, Nayak MK, Dhruwe D et al (2023) Synthesis and characterization of sulfonated magnetic graphene-based cation exchangers for the removal of methylene blue from aqueous solutions. Ind Eng Chem Res 62:1245–1256. https://doi.org/10.1021/acs.iecr.2c04432
23. Kaur K, Title Jindal R (2018) Synergistic effect of organic-inorganic hybrid nanocomposite ion exchanger on ion exchange capacity, Photocatalytic degradation of Rhodamine-B dye and heavy metal ion removal from industrial effluents. J Environ Chem Eng 6(6):7091–7101
24. Rahman MS, Hasan MS, Nitai AS et al (2021) Recent developments of carboxymethyl cellulose. Polymers (Basel) 13. https://doi.org/10.3390/polym13081345
25. Challa R, Ahuja A, Ali J, Khar RK (2005) Cyclodextrins in drug delivery: an updated review. AAPS PharmSciTech 6(2):E329–E357
26. Singh B, Sharma V, Rajneesh et al (2022) Development of dietary fibers moringa-sterculia gum hydrogel for drug delivery applications. Food Hydrocoll Heal 2. https://doi.org/10.1016/j.fhfh.2022.100095
27. Bhattacharya SB, Das AK, Banerji N (1982) Chemical investigations on the gum exudate from sajna (Moringa oleifera). Carbohydr Res 102:253–262. https://doi.org/10.1016/S0008-6215(00)88067-2

28. Singh B, Sharma V, Rohit and Ajay Kumar (2021) Designing Moringa gum-sterculia gum-polyacrylamide hydrogel wound dressings for drug delivery applications. Carbohydr Polym Technol Appl 2:100062. https://doi.org/10.1016/j.carpta.2021.100062
29. Singh B, Kumar A (2021) Development of dietary fibre moringa gum and polyvinylpyrrolidone based hydrogels for drug delivery application. Food Hydrocoll Heal 1:100008. https://doi.org/10.1016/j.fhfh.2021.100008
30. Ranote S, Musioł M, Kowalczuk M, et al (2022) Functionalized Moringa oleifera gum as pH-responsive nanogel for doxorubicin delivery: synthesis, kinetic modelling and in vitro cytotoxicity study. Polymers (Basel) 14. https://doi.org/10.3390/polym14214697
31. Parwani L, Bhatnagar M, Bhatnagar A et al (2016) Evaluation of Moringa oleifera seed biopolymer-PVA composite hydrogel in wound healing dressing. Iran Polym J (English Ed) 25:919–931. https://doi.org/10.1007/s13726-016-0479-8
32. Singh B, Singh J, Sharma V et al (2023) Functionalization of bioactive moringa gum for designing hydrogel wound dressings. Hybrid Adv 4:100096. https://doi.org/10.1016/j.hybadv.2023.100096
33. Ninan N, Muthiah M, Park IK et al (2013) Pectin/carboxymethyl cellulose/microfibrillated cellulose composite scaffolds for tissue engineering. Carbohydr Polym 98:877–885. https://doi.org/10.1016/j.carbpol.2013.06.067
34. Kaur K, Jindal R, Meenu (2019) Self-assembled GO incorporated CMC and Chitosan-based nanocomposites in the removal of cationic dyes. Carbohydr Polym 225. https://doi.org/10.1016/j.carbpol.2019.115245
35. Hebeish A, Sharaf S (2015) Novel nanocomposite hydrogel for wound dressing and other medical applications. RSC Adv 5:103036–103046. https://doi.org/10.1039/c5ra07076g
36. Yang C, Xu L, Zhou Y et al (2010) A green fabrication approach of gelatin/CM-chitosan hybrid hydrogel for wound healing. Carbohydr Polym 82:1297–1305. https://doi.org/10.1016/j.carbpol.2010.07.013
37. Ghattas A-K, Fischer F, Wick A, Ternes TA (2017) Anaerobic biodegradation of (emerging) organic contaminants in the aquatic environment. Water Res 116:268–295. https://doi.org/10.1016/j.watres.2017.02.001
38. Guerrero-Martínez A, González-Gaitano G, Viñas MH, Tardajos G (2006) Inclusion complexes between β-cyclodextrin and a gemini surfactant in aqueous solution: an NMR study. J Phys Chem B 110:13819–13828. https://doi.org/10.1021/jp0615813
39. Hidayat S, Ardiaksa P, Riveli N, Rahayu I (2018) Synthesis and characterization of carboxymethyl cellulose (CMC) from salak-fruit seeds as anode binder for lithium-ion battery. J Phys Conf Ser 1080. https://doi.org/10.1088/1742-6596/1080/1/012017
40. Khushbu JR (2021) Comparative evaluation for controlled release of amoxicillin from RSM-CCD-optimized nanocomposites based on sodium alginate and chitosan-containing inclusion complexes. Mol Pharm. https://doi.org/10.1021/acs.molpharmaceut.1c00340
41. Singh B, Sharma A, Thakur N, Kumar R (2023) Developing dietary fiber moringa gum based ciprofloxacin encapsulated hydrogel wound dressings for better wound care. Food Hydrocoll Heal 3:100128. https://doi.org/10.1016/j.fhfh.2023.100128
42. Bibby DC, Davies NM, Tucker IG (2000) Mechanisms by which cyclodextrins modify drug release from polymeric drug delivery systems. Int J Pharm 197(1–2):1–11
43. Pessine FBT, Calderini A, Alexandrino GL (2012) Review: Cyclodextrin inclusion complexes probed by NMR techniques. InTech
44. Machín R, Isasi JR, Vélaz I (2012) β -Cyclodextrin hydrogels as potential drug delivery systems. Carbohydr Polym 87:2024–2030. https://doi.org/10.1016/j.carbpol.2011.10.024
45. Higuchi T (1963) Mechanism of sustained-action medication. Theoretical analysis of rate of release of solid drugs dispersed in solid matrices. J Pharm Sci 52:1145–1149. https://doi.org/10.1002/jps.2600521210
46. Ritger PL, Peppas NA (1987) A simple equation for description of solute release II. Fickian and anomalous release from swellable devices. J Control Release 5:37–42. https://doi.org/10.1016/0168-3659(87)90035-6
47. Bayraktar O, Malay Ö, Özgarip Y, Batigün A (2005) Silk fibroin as a novel coating material for controlled release of theophylline. Eur J Pharm Biopharm 60:373–381. https://doi.org/10.1016/j.ejpb.2005.02.002
48. Peppas NA, Sahlin JJ (1989) A simple equation for the description of solute release. III. Coupling of diffusion and relaxation. Int J Pharm 57(2):169–172

49. Das S, Subuddhi U (2013) Cyclodextrin mediated controlled release of naproxen from pH-sensitive chitosan/poly(vinyl alcohol) hydrogels for colon targeted delivery. Ind Eng Chem Res 52(39):14192–14200
50. Kaith BS, Sharma R, Kalia S (2015) Guar gum based biodegradable, antibacterial and electrically conductive hydrogels. Int J Biol Macromol 75:266–275. https://doi.org/10.1016/j.ijbiomac.2015.01.046
51. Kaur K, Jindal R (2019) Exploring RSM-CCD-optimized chitosan-/gelatin-based hybrid polymer network containing CPM–β-CD inclusion complexes as controlled drug delivery systems. Polym Bull 76. https://doi.org/10.1007/s00289-018-2555-z
52. Koley R, Rajkumar K, Sahoo S, Chattopadhyay S (2019) Synthesis and characterization of phenol furfural resin from Moringa Oleifera gum and biophenol and its application in styrene butadiene rubber. Ind Eng Chem Res 58(40):18519–18532. https://doi.org/10.1021/acs.iecr.9b03684
53. Kumar B, Priyadarshi R, Singh S (2020) Nanoporous sodium carboxymethyl cellulose-g-poly (sodium acrylate)/$FeCl_3$ nanoporous sodium carboxymethyl cellulose- g -poly (sodium acrylate)/$FeCl_3$ hydrogel beads: synthesis and characterization. Gels 6(4):49. https://doi.org/10.3390/gels6040049
54. Grewal P, Mundlia J, Ahuja M (2019) Thiol modified Moringa gum – a potential bioadhesive polymer. Carbohydr Polym 209:400–408. https://doi.org/10.1016/j.carbpol.2018.12.100

Authors and Affiliations

Kuljit Kaur[1] · Lakhveer Kaur[1] · Anmol[1] · Mehak Sharma[1] · Rajeev Jindal[2]

✉ Kuljit Kaur
kuljit.kaur@gnauniversity.edu.in; kuljitk.cy.15@nitj.ac.in

[1] School of Natural Sciences, GNA University, Phagwara 144401, Punjab, India

[2] Polymer and Nanomaterials Lab, Department of Chemistry, Dr B R Ambedkar National Institute of Technology, Jalandhar 144011, Punjab, India